

Exploration of a NiFeV multi-metal compositional space for the Oxygen Evolution Reaction

Anagha Usha Vijayakumar¹, Jael George Mathew², Anya Muzikansky¹, Hannah-Noa Barad^{*1}, David Zitoun^{*1}

¹*Department of Chemistry and Bar-Ilan Institute for Technology and Advanced Materials (BINA), Bar-Ilan University, Ramat Gan 5290002, Israel.*

²*Max Planck Institute for Intelligent Systems (MPI-IS), Heisenbergstr. 3, 70569 Stuttgart, Germany*

*e-mail: David.Zitoun@biu.ac.il, *e-mail: hannah-noa.barad@biu.ac.il

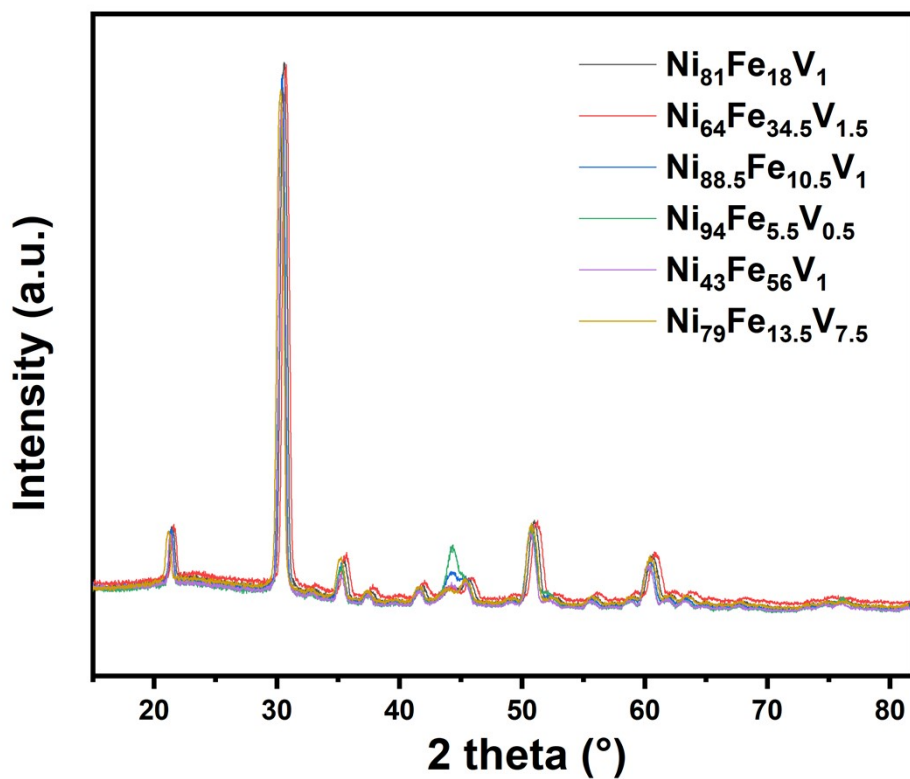


Figure S1. GIXRD of several points on NiFeV library

composition	D spacing (Å°)	Unit cell parameter, a (Å°)
$\text{Ni}_{94}\text{Fe}_{5.5}\text{V}_{0.5}$	2.031	3.517
$\text{Ni}_{88.5}\text{Fe}_{10.5}\text{V}_1$	2.032	3.519
$\text{Ni}_{79}\text{Fe}_{13.5}\text{V}_{7.5}$	2.047	3.545

Table S1. Parameters derived from GIXRD measurements of selected points from NiFeV library. As the added metal level increases, the d-spacing increases, corresponding to a volume expansion due to lattice distortion.

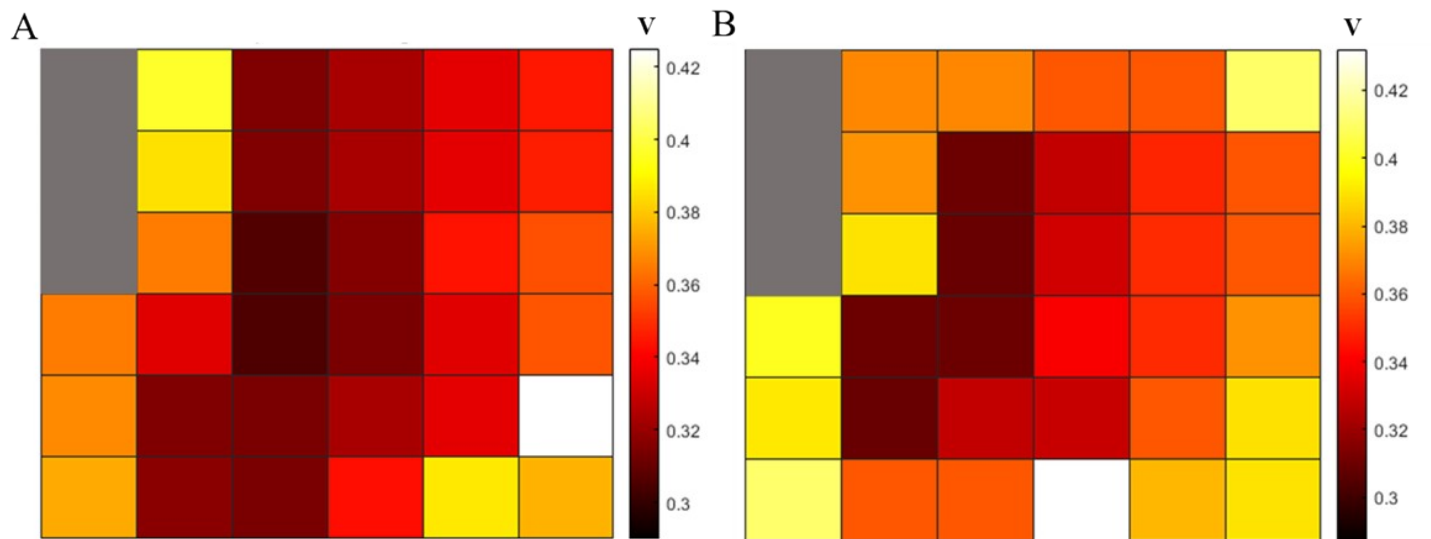


Figure S2. Point by point heatmap of overpotential @10 mA/cm² (A) NiFe library and (B) NiFeV library. The three grey points at the left edge of the map correspond to the points from where contact to the working electrode was placed.

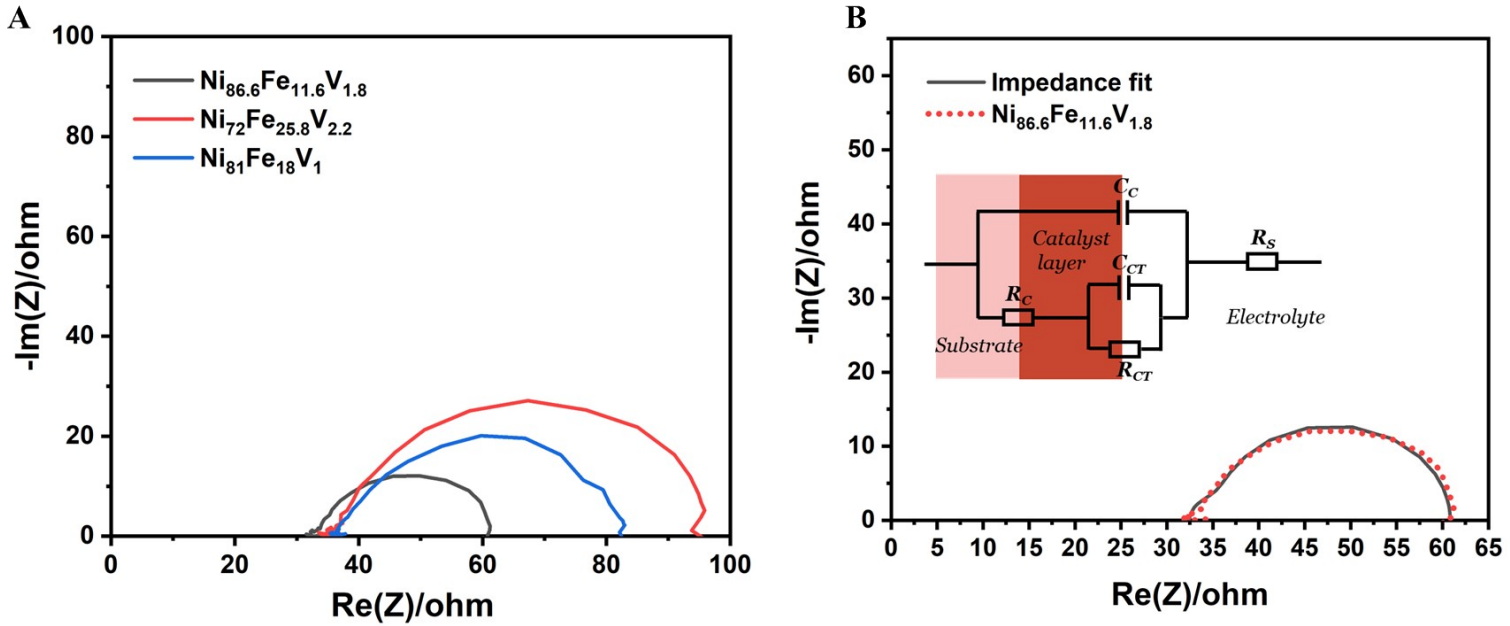


Figure S3. (A) Nyquist impedance of selected points of the NiFeV library. (B) Fitting of the best performing catalyst and the equivalent circuit used for fitting.

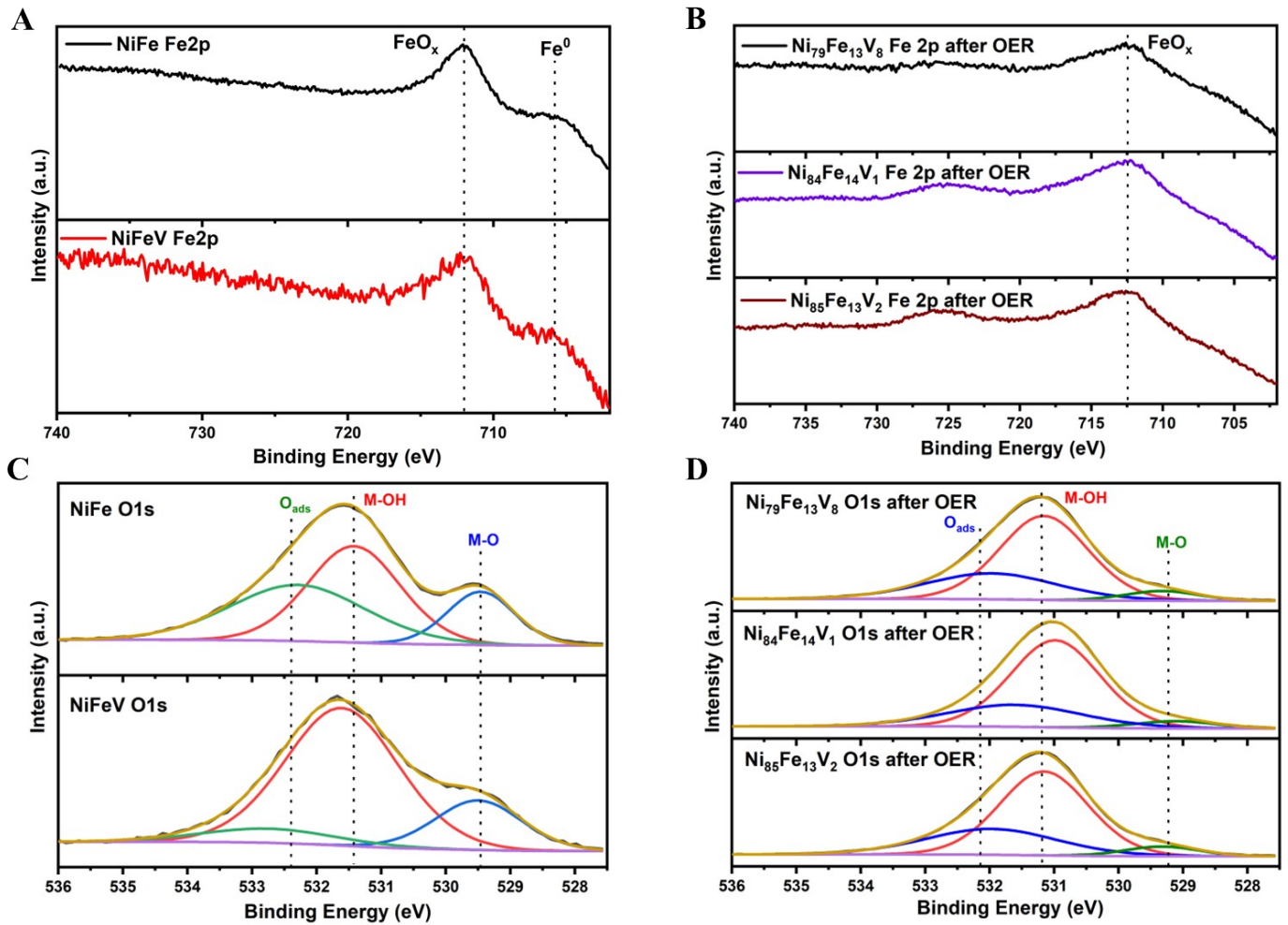


Figure S4. (A) Fe 2p spectra comparison of NiFe and NiFeV before OER (B) Fe 2p spectra comparison of various points on NiFeV after OER (C) O1s spectra comparison of NiFe and NiFeV before OER (D) O1s spectra comparison of various points on NiFeV after OER

Table S2. Comparison of our combinatorial approach vs those from literature

Reference	Combinatorial synthesis route	High throughput screening technique	Comments	Overpotential
Our work	Combinatorial PVD	Automated scanning droplet cell measurements	NiFe and ternary NiFeV libraries	320-330 mV at 10 mA cm ⁻²
H. N. Barad, M. Alarcón-Correa, G. Salinas, E. Oren, F. Peter, A. Kuhn and P. Fischer, <i>Mater. Today</i> , 2021, 50 , 89–99.	Glancing angle PVD	Automated scanning droplet cell measurements	octonary materials libraries consisting of Ni, La, Cr, Mo, BaTi, Co	500 mV -560 mV at 10 mA cm ⁻²
A. U. Vijayakumar, N. Aloni, V. T. Veettil, G. Rahamim, S. S. Hardisty, M. Zysler, S. Tirosh and D. Zitoun, <i>ACS Appl. Energy Mater.</i> , 2022, 5 , 4017–4024.	Spray pyrolysis	Automated scanning droplet cell measurements	NiFeCo oxide library	294 mV – 320 mV at 10 mA cm ⁻²
R. D. Smith, M. S. Prévot, R. D. Fagan, S. Trudel, and C. P. Berlinguette, <i>J. Am. Chem. Soc.</i> , 2013, 135 , 11580–11586.	Photochemical metal–organic deposition (PMOD) (each thin film was deposited individually)	Three electrode electrochemical cell (not automated)	21 different compositions of NiFeCo oxide films were investigated for OER.	210-250 mV at <u>0.5 mA cm⁻²</u>
C. Schwanke, H. S. Stein, L. Xi, K. Sliozberg, W. Schuhmann, A. Ludwig, and K. M. Lange, <i>Scientific reports</i> , 2017, 7 , 1-7	Combinatorial reactive magnetron sputtering	Automated scanning droplet cell measurements	130 elemental compositions of ternary NiFeCrOx library	320 mV at <u>1.15 mA cm⁻²</u>
X. Cao, E. Johnson and M. Nath, <i>ACS Sustain. Chem. Eng.</i> , 2019, 7 , 9588–9600.	Combinatorial electrodeposition	Three electrode electrochemical cell (not automated)	66 different compositions of quaternary Fe-Co-Cu selenides	256 mV at 10 mA cm ⁻²

Table S3. Comparison of our NiFeV catalyst with those from literature

Reference	Synthesis method	Catalyst composition	Overpotential at 10 mAcm ⁻²	Tafel slope (mV dec ⁻¹)

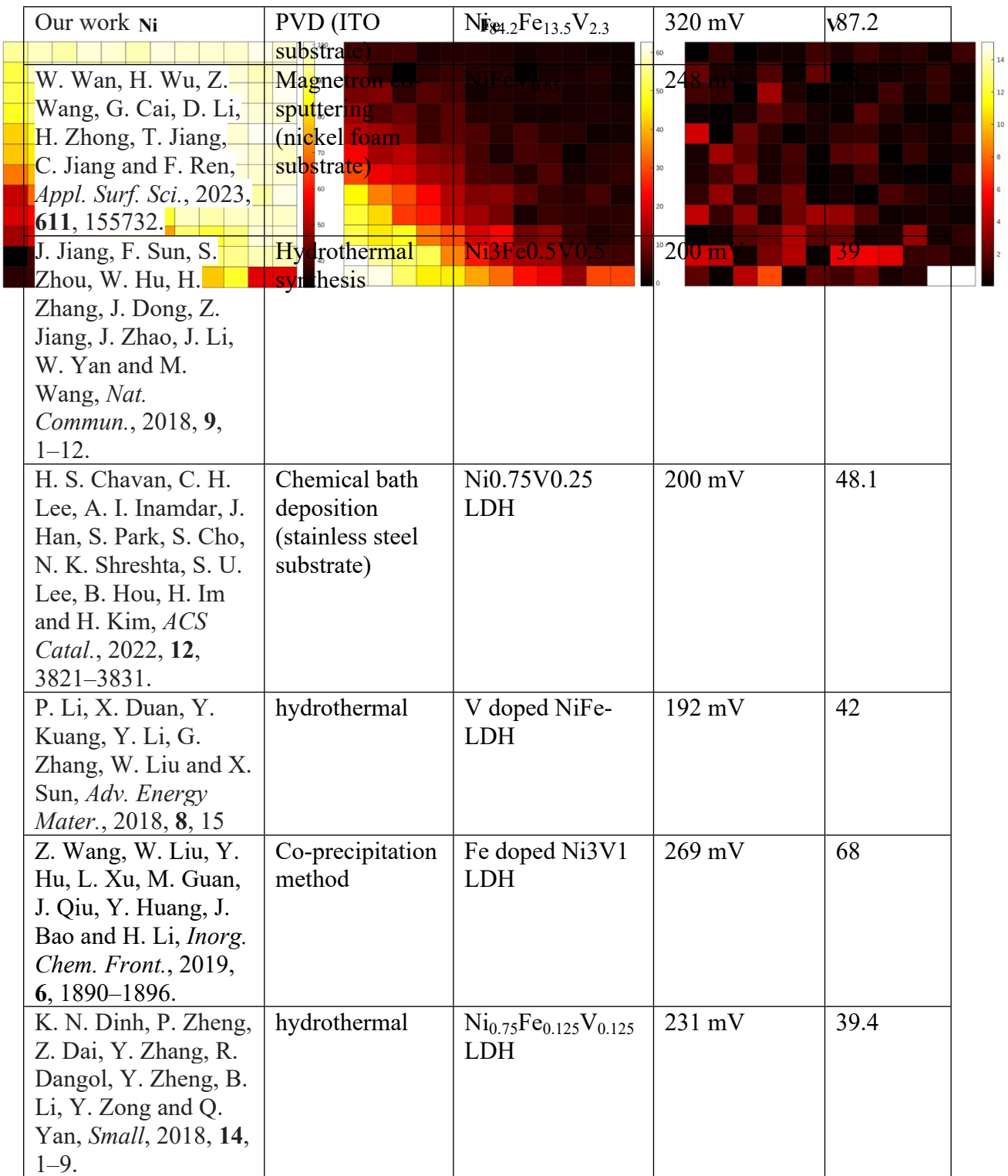


Figure S5. EDAX measurements on NiFeV sample

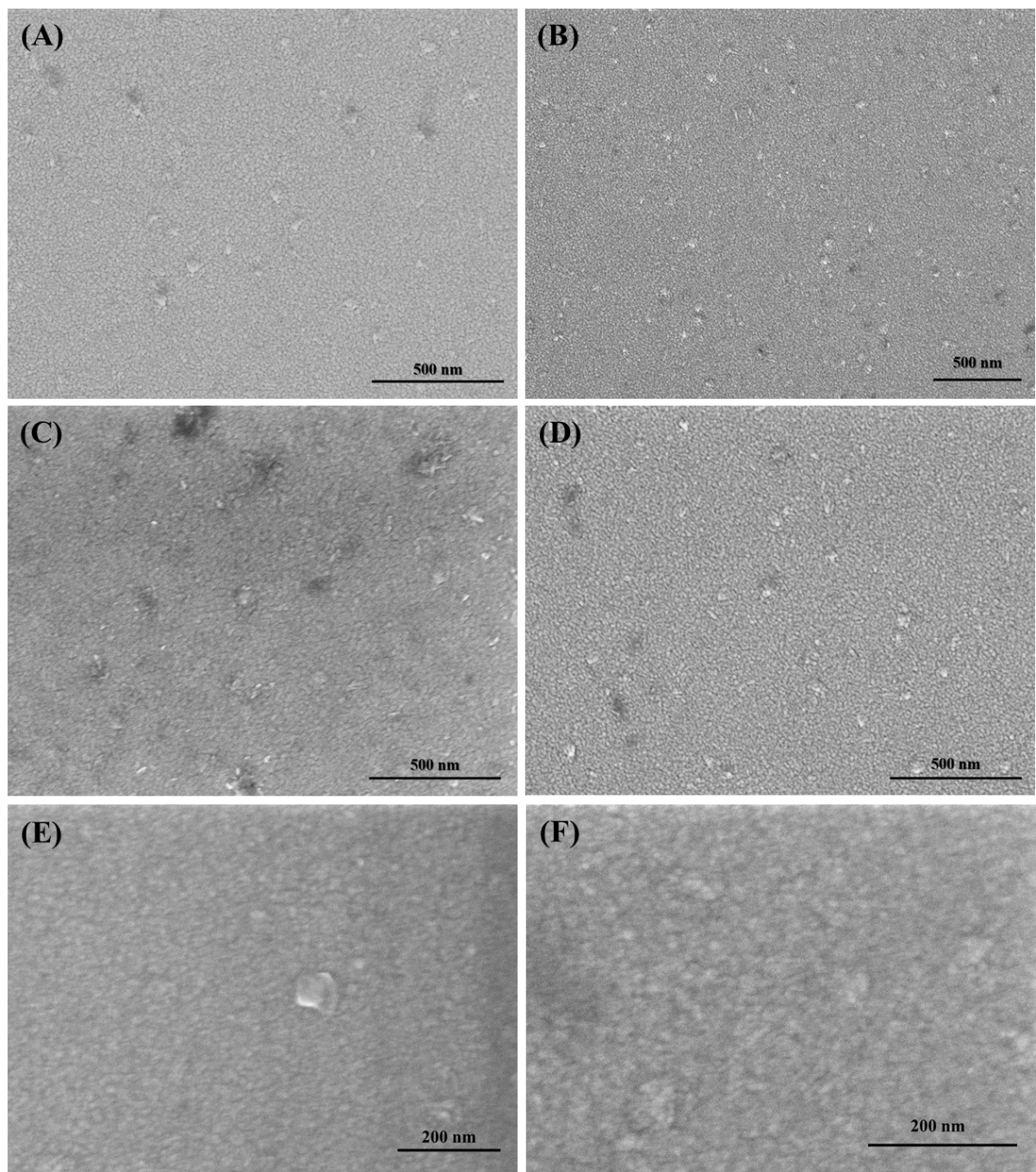


Figure S6. HRSEM measurements at different points on NiFeV sample.

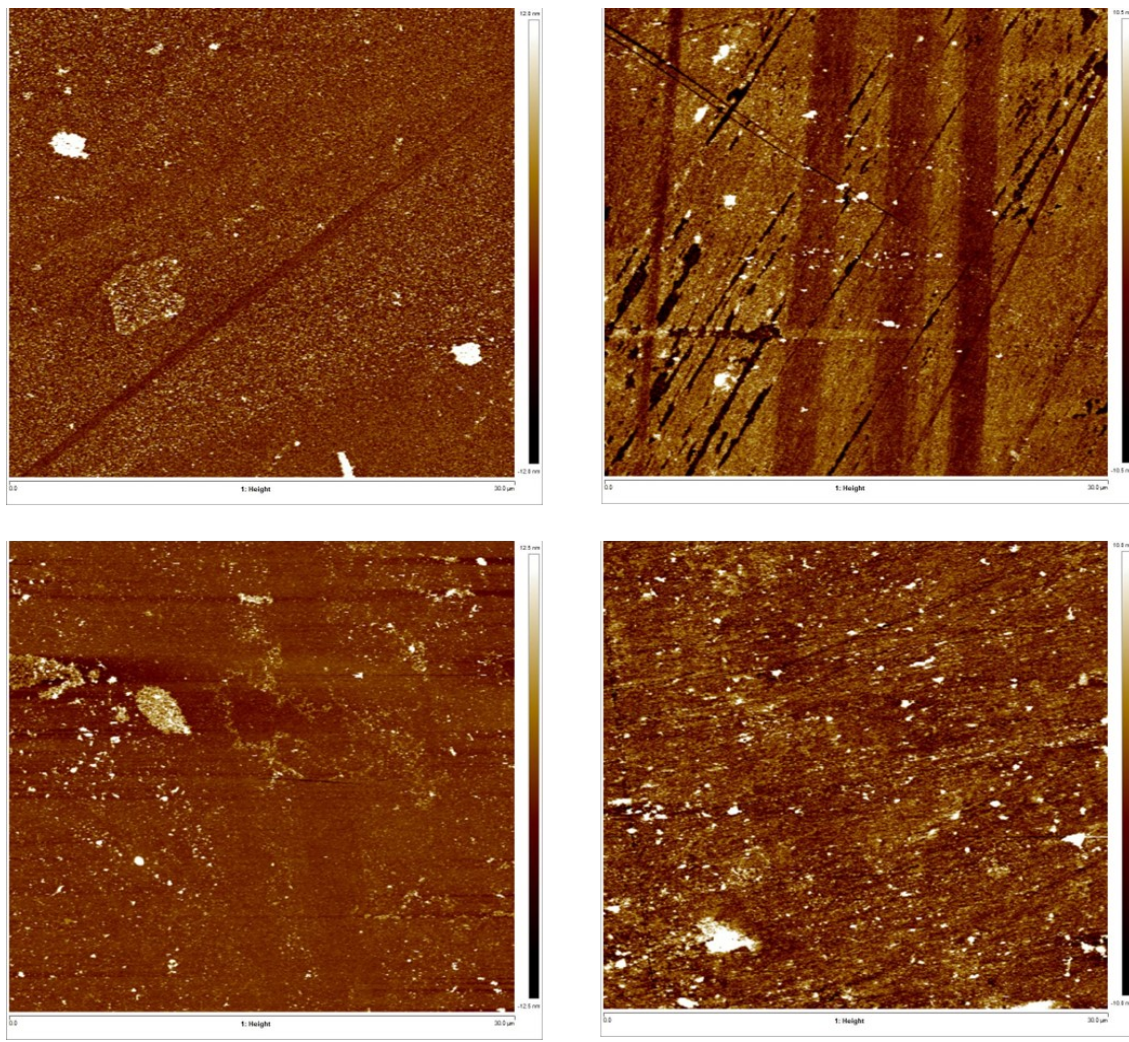


Figure S7. AFM images ($30 \times 30 \mu\text{m}$) taken at various points on the NiFeV thin film.

Sample	R_a (nm)
Point 1	1.84
Point 2	2.02
Point 3	1.14
Point 4	2.03

Table S4. Calculated surface roughness (r_a) at various points on the NiFeV thin film

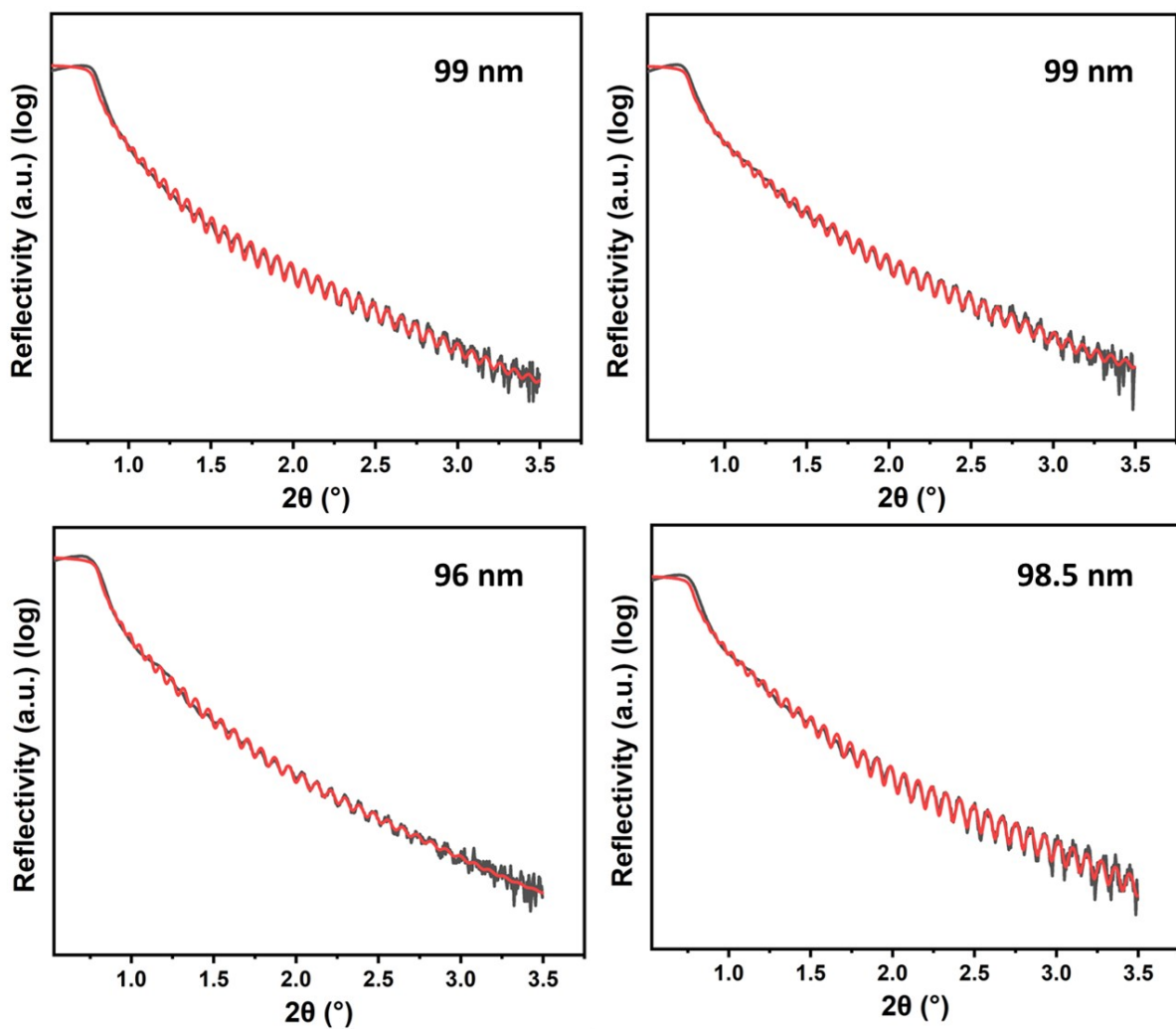


Figure S8. XRR measurements at various points on the NiFeV sample.

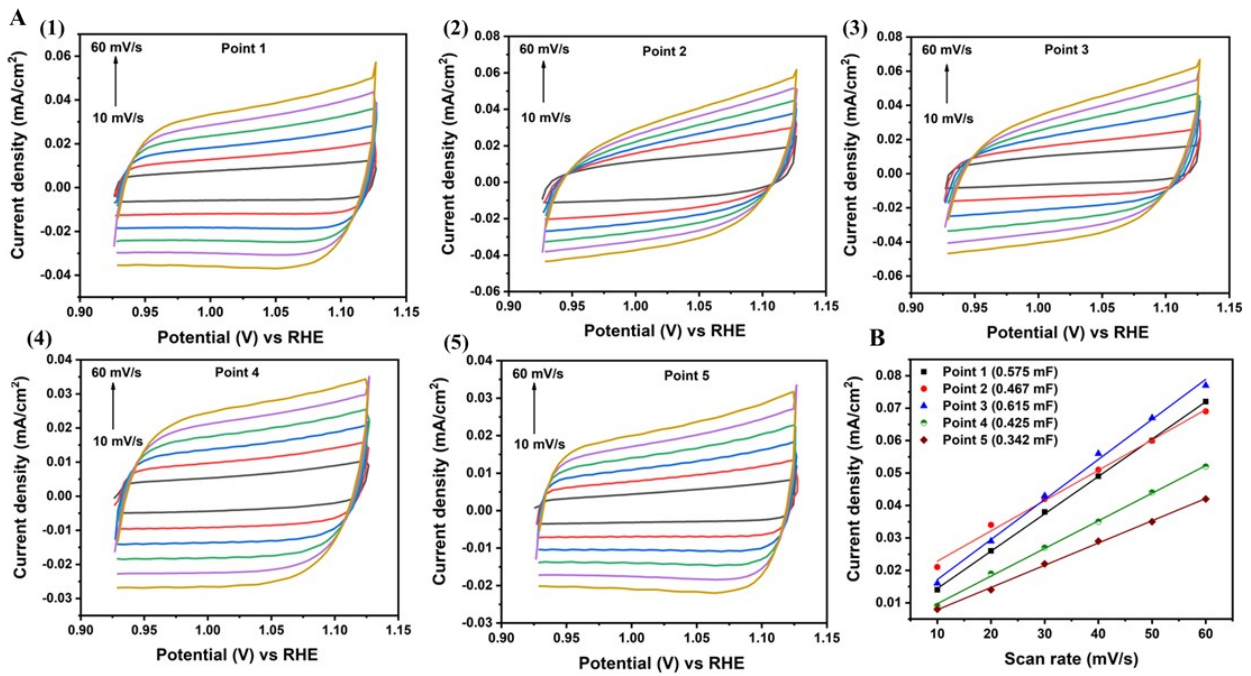


Figure S9.(A) CV measurements in the non-faradaic region at various points on the NiFeV sample (B) Scan rate vs current density plot at all measured points for Cdl calculation from slope

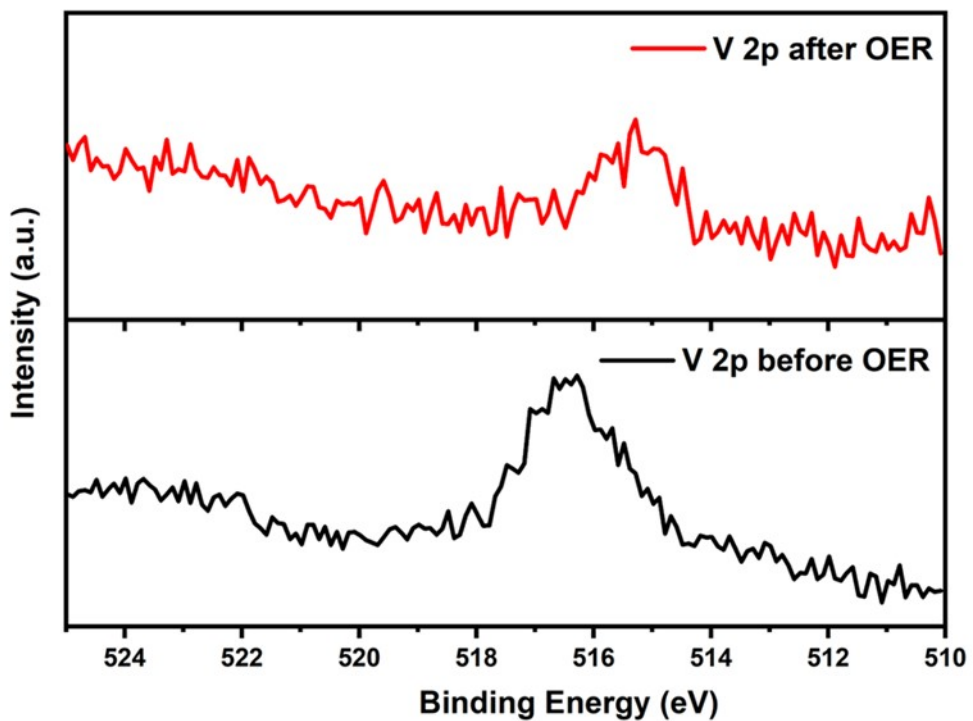


Figure S10. V2p XPS spectrum of NiFeV before and after OER measurement.